Contribution of Lignin from Different Bioresources to the Pollution Load

Zhimin Wei, Youming Li, Fengjian Cai, and Yi Hou *

Lignin was extracted from eucalyptus, *Pinus koraiensis*, and bagasse (representatives for hardwood, softwood, and Gramineae, respectively) black liquors to quantitatively distinguish the pollution loads caused by lignin. The results indicated that the actual common chemical oxygen demand (COD_{Cr}) of lignin was lower than the theoretical COD_{Cr} with an actual oxidative ratio of approximately 85%. The results also showed that 1 kg of lignin from eucalyptus, *P. koraiensis*, and bagasse could produce COD_{Cr} pollution loads of 1.476 kg, 1.540 kg, and 1.561 kg, respectively, which revealed the large contribution of lignin to the pollution load. Through the elemental analysis, infrared spectroscopy, and nuclear magnetic resonance analysis in the hydrogen and carbon spectra of the different lignin, it was found that guaiacyl structures in the lignin units can lead to a better thermal stability for *P. koraiensis*. Compared with the *P. koraiensis* and bagasse lignins, the eucalyptus lignin had a higher elemental oxygen content and lower molecular weight with mainly syringyl structures, which resulted in a higher reaction activity.

Keywords: Lignin; Structure; Chemical oxygen demand (COD)

*Contact information: State Key Laboratory of Pulp and Paper Engineering, South China University of Technology, Guangzhou 510640, China; * Corresponding author: ceyhou@scut.edu.cn*

INTRODUCTION

The pulp and paper industry is facing increasingly more stringent effluent limitations in China (Lei *et al.* 2013; Salem and Böhm 2013). Lignin is an important component of wood, and its degradation products, which originate from cooking and bleaching processes, are major wastewater contaminants (Martínez *et al.* 2005; Kumar *et al.* 2009). Past research has focused on wastewater treatment processes and lignin applications. For example, Lucas *et al.* (2012) studied Fenton oxidation technology and found that under the same experimental conditions, the sunlight-Fenton reaction is more effective than the corresponding dark reaction, which brings about the mineralization of the dissolved organic carbon (DOC), and the removal rate of chemical oxygen demand (COD) and total phosphorus (TP) is higher than 90% (Lucas *et al*. 2012). Laurichesse *et al.* (2014) reacted the solvent lignin with oil, and then they cyclized the double bond in oleic acid. A lignin-oleic acid polyhydroxy polymer (LOAP) was synthesized by an oxidation reaction and a ring-opening reaction (Laurichesse *et al.* 2014).

Lignin is the main source of pollution in pulp and papermaking wastewater. However, there has been no relevant research on the quantitative influences of the lignin structure on the pollution load because of its complex amorphous structure. The chemical oxygen demand is an important parameter for the determination of the pollution load in water (Barker *et al.* 1999; Bansode *et al.* 2004). The detailed estimation of pollution of

lignin will helps to identify the amount of pure COD in wastewater and the cost of removing pure COD emission sources and leads to control and/or reduce their production.

The aim of the present work was to study the contribution of lignin to the COD content, which will provide basic data for the design of wastewater treatment processes and environmental protection in the pulp and paper industry. It is very important to effectively control and provide wastewater online monitoring and optimization by quantitative research on lignin, which could assist the industry to protect the environment and provide financial benefits. Black liquors from *Pinus koraiensis* (softwood), eucalyptus (hardwood), and bagasse (Gramineae) were used as the raw materials to extract lignin. The COD values of the three lignin samples were measured, which was followed by elemental analysis, gel permeation chromatography (GPC), thermogravimetric analysis (TGA), and spectral analysis, including Fourier transform infrared (FT-IR) spectroscopy, proton nuclear magnetic resonance (^{1}H-NMR), and carbon-13 NMR (^{13}C-NMR), to characterize the structure.

EXPERIMENTAL

Materials

All of the chemicals involved in this study are commercially available and were used as received without further purification. Deionized water was used in all of the experimental procedures.

Methods

Preparation and purification of the alkali lignins

The black liquors from the *P. koraiensis*, eucalyptus, and bagasse were made in the laboratory according to the traditional alkali cooking method. Separation and purification of the alkali lignin samples were performed according to the method by Wu *et al.* (2008).

Elemental analysis

The elemental analysis was performed to determine the carbon, hydrogen, oxygen, and nitrogen contents in the lignin samples using a Vario EL III analyzer (Elementar, Frankfurt, Germany).

Thermogravimetric analysis

The thermal decomposition characteristics of the alkali lignins were determined with a Q-500 IR instrument (TA Instruments, Newcastle, USA). The TGA was performed at a constant heating rate of 10 °C/min, up to 600 °C. An inert N_2 atmosphere was maintained with a flowrate of 30 mL/min.

Gel permeation chromatography

The lignin was acetylated with acetic anhydride/pyridine (2:1 v/v) at room temperature for 72 h, and the derivatized lignin was dissolved in tetrahydrofuran. The lignin was then analyzed using a GPC max instrument (Waters 515, Agilent, Milford, USA) equipped with a PLgel 5 μm MIXED-D column (300 mm × 7.5 mm) (Agilent). To determine the molecular weight of the effluent, polystyrenes with a mass range of 1000 Da to 500000 Da were used to create a calibration curve.

Spectroscopic analysis (FT-IR, ^{1}H-NMR, and ^{13}C-NMR)

The FT-IR spectra were recorded on a Tensor 27 spectrometer (Bruker, Karlsruhe, Germany) operating in the wavelength range of 4000 cm^{-1} to 400 cm^{-1} with a resolution better than 0.50 cm^{-1}. Each sample was coated with potassium bromide (KBr) and formed into a pellet for analysis. The ^{13}C-NMR and ^{1}H-NMR spectra were obtained using a Bruker AVIII 400 spectrometer (Bruker) that was operated at 25 °C using 30000 (^{13}C-NMR) and 130 (^{1}H-NMR) scans with 160 mg of lignin sample dissolved in DMSO-d_6.

Determination of the chemical oxygen demand

One gram of refined lignin was weighed and dissolved in 50 mL of dinitrosalicylic acid (DNS) solution at room temperature to prepare a lignin standard solution with a concentration of 2 g/L. Fifty milliliters of DNS solution were taken at room temperature, and its volume was adjusted to 500 mL with deionized water. A DNS standard solution was prepared to eliminate the contribution of the DNS solution to the COD. The determination of the COD was performed using a spectrophotometer (DR2800, Hach, Loveland, USA), according to standard methods (Karichappan *et al.* 2014).

RESULTS AND DISCUSSION

Table 1 shows the elemental composition and C_9 formula of the three lignin samples extracted from the black liquors and purified with 1,4-dioxane. The elemental carbon and oxygen contents of the three lignins were relatively high (C: 62.2%, 60.12%, and 62.26%; O: 31.92%, 34.33%, and 31.53%), and were determined by the C_9 structure of the lignin. At the same time, the atomic ratio of C to H was high, which indicated that the aromatic rings content in the alkali lignins was high. The proportion of oxygen was also high, which indicated that there were many hydroxyl, methoxy, and ether bonds in the alkali lignins (Canadian Journal of Chemical Engineering 1987; Asmadi *et al*. 2011a,b; Huang *et al*. 2013).

Table 1 shows that the oxygen content of the eucalyptus lignin was remarkably higher than that of the *P. koraiensis* and bagasse lignins. This distinction may have been a result of the structural differences in the lignin structural unit in the raw materials, which can be seen in Fig. 1. Eucalyptus, a hardwood raw material, contains mainly syringyl (S-type) and guaiacyl (G-type) structural units, with S-type structural units being more prevalent (Santos *et al.* 2012; Ohra-aho *et al.* 2013). The methoxy (-OCH_3) content in the S-type structural units is higher than in the G-type and p-hydroxyphenyl (H-type) structural units, which contributed to the higher oxygen content. This can be inferred that the oxygen content is closely related to COD.

Table 1. Elemental Analysis and C_9 Empirical Formula of the Alkali Lignins

Lignin	C (%)	H (%)	O (%)	N (%)	C/H Ratio	C_9 Formula
P. koraiensis	62.270	5.762	31.918	0.050	10.807	$C_9H_{9.99}O_{3.46}N_{0.006}$
Eucalyptus	60.120	5.522	34.328	0.030	10.888	$C_9H_{9.92}O_{3.85}N_{0.004}$
Bagasse	62.260	5.959	31.531	0.250	10.447	$C_9H_{10.34}O_{3.42}N_{0.03}$

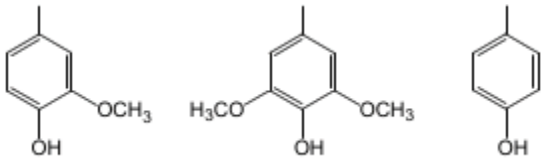

Fig. 1. Structural lignin units

The DNS solution was used as a solvent to determine the effects of lignin on the common COD (COD_{Cr}). Using the lignin concentration as the Y-axis and the COD_{Cr} as the X-axis, the correlation between the lignin concentration and COD_{Cr} was obtained (Fig. 2). Figure 2 shows that the correlation coefficient of the linear regression equation was close to 1, which indicated a strong linear relationship. According to the slope of the standard curves, it was found that 1 kg of the eucalyptus, *P. koraiensis*, and bagasse lignins produced 1.476 kg, 1.540 kg, and 1.561 kg of COD_{Cr}, respectively, which showed the large contribution to pollution by lignin. It was observed that the eucalyptus had the smallest COD value and the bagasse the largest. Eucalyptus is a hardwood, and its lignin is mainly composed of S-type structural units. Bagasse is a member of Gramineae, and that plant family mainly contains lignin having an H-type structure. As shown in Fig. 1, the S-type structure has a higher oxygen content than the H-type structure, which may be the cause of the minimum COD value of the eucalyptus. COD, chemical oxygen demand, is a chemical method for measuring the amount of oxygen consumed by an organic compound in a water sample when it is oxidized by a strong oxidant. It can be inferred by definition that the higher the oxygen content, the lower the COD value will be.

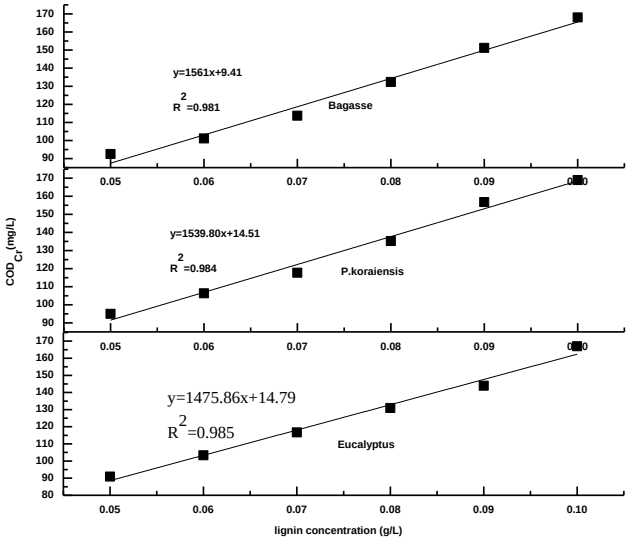

Fig. 2. Alkali lignin concentration and COD_{Cr} content relation curve

The theoretical COD, which is the amount of oxygen required to completely oxidize organic compounds to carbon dioxide (CO_2) and water (H_2O), was calculated stoichiometrically, based on the chemical formula of the organic compounds:

$$C_aH_bO_c + (a + (b/4) - (c/2))O_2 \rightarrow aCO_2 + (b/2)H_2O \quad (1)$$

a: The amount of C atoms； b: The amount of H atoms;c: The amount of O atoms.

Then, the theoretical COD was determined using the following formula:

$$\text{Theoretical } COD = \frac{\left(a + \frac{b}{4} - \frac{c}{2}\right) \times 32}{a \times 12 + b + c \times 16} \text{ (g/g)} \quad (2)$$

Using the elemental analysis of the lignin and the C_9 formula, the theoretical COD values of the different lignin samples were estimated. Table 2 shows that 1 kg of the eucalyptus, *P. koraiensis*, and bagasse lignins should produce theoretical COD values of approximately 1.703 kg, 1.803 kg, and 1.826 kg, respectively. When compared with the actual COD_{Cr}, the value of the theoretical COD was larger because lignin macromolecules are too complex to be completely oxidized. Therefore, the actual and theoretical COD_{Cr} values obtained by combining this experimental method can reflect the actual oxidation rate of alkali lignin.

Among the three kinds of alkali lignin, the actual oxidation rate of the eucalyptus lignin was higher because it has mostly S-type structural units. It is known to have a methoxy group that has an electron donating effect on the aromatic ring, which could easily activate the aromatic ring and make the lignin more prone to oxidation and degradation (Britt *et al*. 2007; Parthasarathi *et al*. 2011). Moreover, the cleavage of methyl-aryl ether bonds during alkaline cooking produces methanol, methyl mercaptan, *etc*., so that the degradation degree of the side chain on the aromatic ring structure during the preparation of eucalyptus lignin was greater than that during preparation of the *P. koraiensis* and bagasse lignins. It was found that the composition of the S-type structural unit was more easily degraded or oxidized in a chemical reaction with a higher oxidation ratio. The theoretical calculation of lignin, in combination with the actual oxidation rate, will provide an online simulation data basis for the contribution of the main pollution source of pulp and paper to COD.

Table 2. Contribution of Lignin to the COD

Lignin	Theoretical COD (g/g)	COD_{Cr} (g/g)	Actual Oxidation Rate (%)
P. koraiensis	1.803	1.540	85.41
Eucalyptus	1.703	1.476	86.67
Bagasse	1.826	1.561	85.49

The average molecular weights (M_w and M_n) and polydispersity index of the three lignin samples were determined using GPC analysis, and the results are given in Table 3. The M_w values were determined to be 12062 Da, 5493 Da, and 8849 Da for the *P. koraiensis*, eucalyptus, and bagasse lignins, respectively. The results showed that the chemical bonds between the monomers in the lignin structure, such as the α aryl ether, β aryl ether, and C-C bonds, were destroyed to a major degree during alkaline cooking, which resulted in a remarkable reduction in the molecular weight of the alkali lignin. The molecular weight of the eucalyptus lignin was the smallest, which may have been a result of the destruction of more chemical bonds in the lignin structure during the cooking process. Compared with the *P. koraiensis* and bagasse alkali lignins, high contents of S-type structural units in the eucalyptus lignin resulted in a higher methoxy ($-OCH_3$) content. Additionally, the methoxy group on the aromatic ring was easily destroyed by the alkaline

solution in the cooking process, and the -OCH_3 group could interact with other functional groups, such as the hydroxyl group on the side chain, which reduced the dissociation energy of the C_β-O bond and made it easier for the lignin structure to be decomposed in the alkali solution (Rohella *et al.* 1996; Pasquali and Herrera 1997; Ghaffar and Fan 2014). However, while the *P. koraiensis* lignin was mainly composed of G-type units, the G-type structure is relatively stable in the process of cooking, which made its molecular weight relatively large.

Table 3. Average Molecular Weight and Polydispersity Index of the Alkali Lignins

Lignin	M_w (Daltons)	M_n (Daltons)	M_w/M_n
P. koraiensis	12062	6360	1.90
Eucalyptus	5493	3395	1.62
Bagasse	8849	5361	1.65

Polydispersity index – M_w/M_n

The TGA and differential thermogravimetric (DTG) curves of the three lignins are given in Fig. 3. From the DTG curves, the maximum decomposition rate (V_m) of the *P. koraiensis* was 0.35%/°C, while that of the eucalyptus and bagasse were 0.31%/°C and 0.38%/°C, respectively. The temperature (T_m) corresponding to the V_m shifted to a lower temperature region (T_m = 377.42 °C) for the *P. koraiensis* compared with that of the eucalyptus (330.9 °C) and bagasse (355.8 °C). Furthermore, the active pyrolysis region of the *P. koraiensis* was from 100 °C to 377.4 °C, whereas it was from 100 °C to 330.9 °C and from 100 °C to 355.8 °C for the eucalyptus and bagasse, respectively. The active pyrolysis region is defined as the thermal degradation region from approximately 100 °C (dehydration step) to the T_m as determined from the V_m in the DTG curve (Hodgson *et al.* 2011). These results suggested that *P. koraiensis* was more thermally stable than the eucalyptus and bagasse, as was evident from the higher T_m for the *P. koraiensis*. The thermal stability of lignins increase with incrementally higher M_w values.

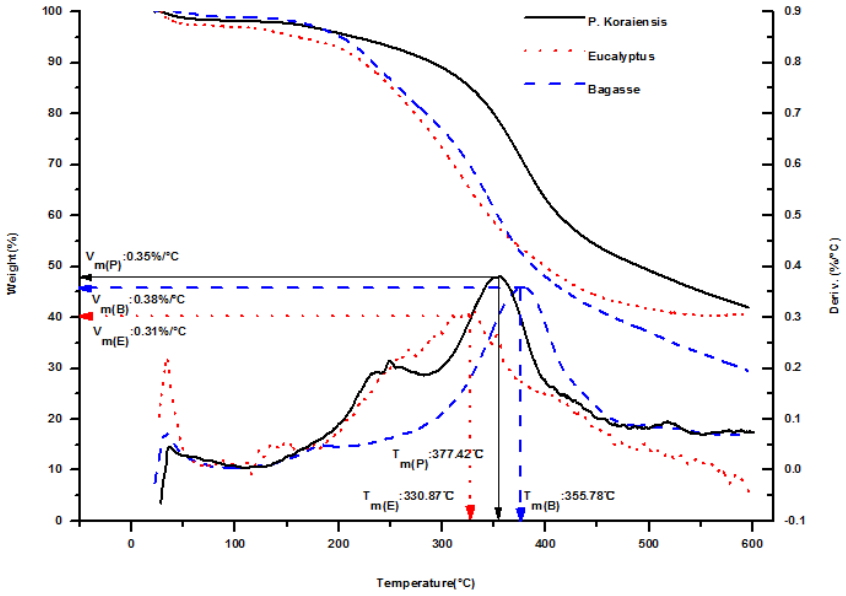

Fig. 3. TGA and DTG curves of the alkali lignins

With a greater degree of branching and condensation of the lignin macromolecule, the thermal energy needed for bond cleavage increases (Sun *et al.* 2000). This may be because the No. 5 position of the S-type structural unit is occupied by -OCH_3, and the G unit is liable to form a C-C bond structure. Due to the high stability of this stable structure, complete fracture does not occur at the time of extraction of the alkaline solution. Therefore, it is presumed that the *P. koraiensis* component contains more C-C bond structural units, and its stability is stronger than that of the S-type structural unit. It can be inferred that the G-type unit polylignin has a relatively high thermal stability.

For an in-depth clarification of the structural features of lignin molecules, the three alkali lignins were also subjected to FT-IR spectroscopic analyses. The representative spectra are shown in Fig. 4 and Table 4. Figure 4 shows that the FT-IR spectra for the three lignins appeared to be almost identical, and typical lignin peaks, such as O–H stretching (3412 cm^{-1} to 3460 cm^{-1}), C–H stretching of methyl/methylene groups (3000 cm^{-1} to 2842 cm^{-1}), aromatic skeletal vibrations (1505 cm^{-1} to 1515 cm^{-1}), and aromatic C–H in-plane deformation (1200 to cm^{-1} 1000 cm^{-1}), were visible in all of the spectra. These strong absorption peaks indicate that the different lignin structures extracted by the alkaline solution are similar. These findings indicate that the "core" structure of the lignin was not destroyed, such as the typical lignin infrared absorption peak was exhibited.

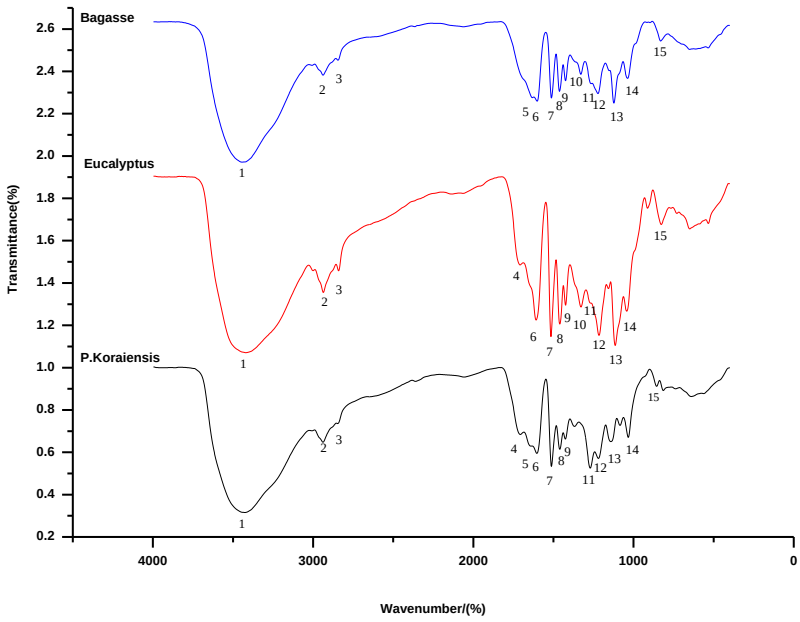

Fig. 4. FT-IR spectra of the alkali lignins

However, in contrast, there were differences between different lignins, 1714 cm^{-1} and 1716 cm^{-1} are the stretching vibration absorption of non-co-anthracene, carbonyl and ester bonds and C=O conjugate, respectively, in eucalyptus and bagasse lignin. The absorption peaks at 1714 cm^{-1} and 1716 cm^{-1} were sequentially enhanced, while the absorption peaks in the *P. koraiensis* lignin were relatively low. On the contrary, the bagasse lignin showed a strong absorption peak at 1641 cm^{-1}. It is indicated that the alkaline

solvent extraction can retain the conjugated C=O group in the acetate, ferulic acid, and acid in the baggage lignin structure, while the alkaline solution extraction leads to the breakage of the group in eucalyptus lignin. 1328 cm^{-1} is the C-O absorption of S-type unit lignin, and 1271 cm^{-1}, and 1269 cm^{-1} are G-type lignin C-O and C=O absorptions. It can be seen from the figure that *P. koraiensis* lignin contains more G-type structure.

Table 4. Results of the IR Bands for the Alkali Lignins

Serial No.	Band Position (cm^{-1})			Assignment
	P. koraiensis	Eucalyptus	Bagasse	
1	3425	3433	3452	O-H stretching
2	2939	2933	2939	C-H stretching
3	2841	2839	2842	C-H stretching
4	1714	1716	—	C=O stretching (unconjugated)
5	1650	—	1641	C=O stretching (conjugated)
6	1604	1608	1598	Aromatic skeletal vibration + C=O stretching
7	1512	1515	1510	Aromatic skeletal vibration
8	1460, 1365	1460	1463	C-H deformation (methyl and methylene)
9	1423	1423	1423	C-H in-plane deformation with aromatic ring stretching
10	—	1328	1328	C-O of syringyl (S) ring
11	1272	1269	1269	C-O of guaiacyl (G) ring + C=O stretching
12	1217	1215	1222	C-C + C-O + C=O stretching
13	1136, 1087	1114	1122	Guaiacyl C-C, C-O and syringyl C-C, C-O + C-O deformation of secondary alcohols and aliphatic ethers
14	1031	1037	1035	Aromatic C-H in-plane deformation (G > S)
15	858	823	831	Aromatic C-H Bending vibration

For the ^{13}C-NMR spectra (Fig. 5 and Table 5), most of the lignin signals, such as the aromatic carbons at 100 ppm to 155 ppm, aliphatic side chain carbons at 86 ppm to 60 ppm, and the methoxyl carbon at 56.4 ppm, appeared equally in the three alkali lignin spectra. Meanwhile, the arylglycerol-β-aryl ether linkage (β-O-4) is considered to be a typical linkage type in lignin macromolecules. Figure 5 shows that the side chain C-α, C-β, and C-γ on the β-O-4 bond appeared to have signal peaks at 73 ppm to 75 ppm, 86 ppm, and 61.7 ppm to 65 ppm, respectively.

Additionally, some similarities were seen in the ^{1}H-NMR spectra (Fig. 6 and Table 6). There were aromatic hydrogens at 6.4 ppm to 7.8 ppm, H_β in the β–β structures at 3.2 ppm to 3.5 ppm, *etc*. (Capanema *et al.* 2004; Vanholme *et al.* 2010). The chemical shift between 6.0 and 8.0 ppm is derived from the signals of the G and S type lignin aromatic rings, while 0.8 to 1.5 ppm is the signal of the hydrogen atoms on the aliphatic functional groups. Specifically, the absorption peak at 6.7 ppm or 6.8 ppm represents the absorption

of G-type lignin, and the absorption peak at 6.6 ppm is the absorption peak of the S-type lignin unit. The weaker signal at 6.6 ppm of *P. koraiensis* indicates that the *P. koraiensis* lignin contains no or a small amount of S-type lignin units. 3.7 ppm and 3.8 ppm are derived from methoxy groups. Further, 4.9 ppm represents the signal of the β-position hydrogen proton of the lignin β-O-4 aryl ether unit, and the signal at 4.3 ppm is derived from the signal of the γ-position hydrogen proton of the lignin β-O-4 aryl ether unit structure.

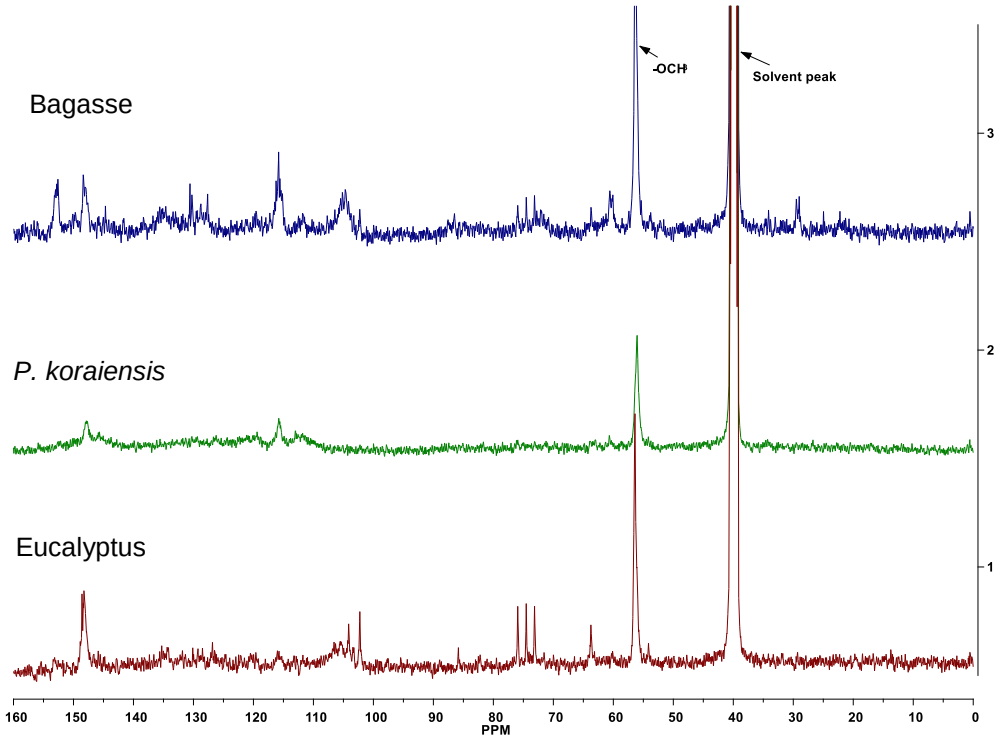

Fig. 5. ^{13}C-NMR spectra of the alkali lignins

Table 5. Assignment of the ^{13}C-NMR Bands for the Alkali Lignins

Serial No.	Signal (ppm)			Assignment
	P. koraiensis	Eucalyptus	Bagasse	
1	-	-	153	C_3/C_5 of β-O-4 in H units
2	148	147	148	C_3 and C_4 in G units
3	-	-	138.5	C_4 in in S units
4	-	135	135	C_1 in in S units
5	-	-	130	C_2 and C_5 in H units
6	127	127	128	Cα=O in G units
7	-	119	119	C_3 and C_5 in H units
8	116	116	116	C_5 in G units
9	-	105	105	C_2 and C_5 in S units
10	-	86	86	C-β
11	-	75 - 73	75 - 73	C-α
12	65 - 61.7	65 - 61.7	65 - 61.7	C-γ
13	56.4	56.4	56.4	$-OCH_3$
14	34 - 20	34 - 20	34 - 20	Saturated aliphatic chains

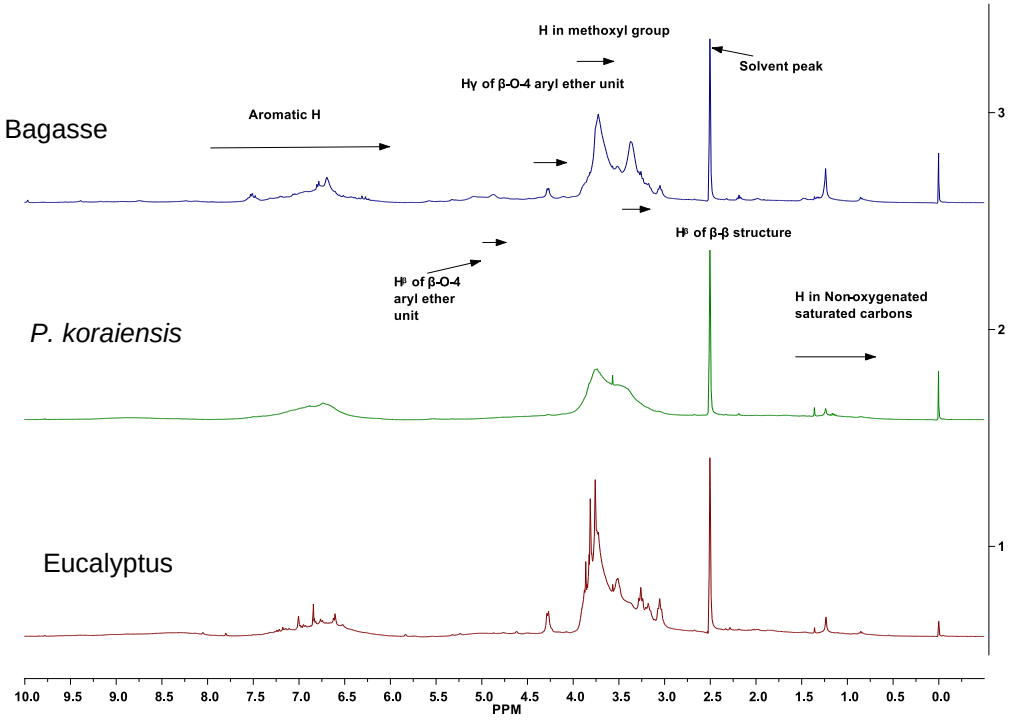

Fig. 6. ^{1}H-NMR spectra of the alkali lignins

Table 6. Assignment of the ^{1}H-NMR Bands for the Alkali Lignins

Signal (ppm)	Signal (ppm)			Assignment
	P. koraiensis	Eucalyptus	Bagasse	
7.8 - 7.47	-	-	7.5	Aromatic H in H units
7.47 - 6.7	6.8	6.7	6.8	Aromatic H in G units
6.7 - 6.4	-	6.6	6.69	Aromatic H in S units
5.4 - 4.6	-	-	4.9	H_β of β-O-4 aryl ether unit
4.5 - 4.0	4.3	4.3	4.3	H_γ of β-O-4 aryl ether unit
4.0 - 3.5	3.8	3.8	3.7	H in methoxyl group
3.5 - 3.2	3.3	-	3.4	H_β of β-β aryl ether unit
3.2 - 3.0	-	3.1	3	H in methoxyl group
2.5	2.5	2.5	2.5	DMSO
1.45 - 0.7	1.4	1.2	1.2	H in non-oxygenated saturated carbons

CONCLUSIONS

1. Different sources of lignin have different pollution contributions to the environment, which is an important quantitative comparison. Accordingly, 1 kg of lignin from eucalyptus, *P. koraiensis*, and bagasse could produce COD_{Cr} pollution loads of 1.48 kg, 1.54 kg, and 1.56 kg, respectively, because of the difference in the structural units. The actual COD_{Cr} of the lignin was lower than the theoretical COD_{Cr}, with an actual oxidative ratio of approximately 85%.

2. The G-type structures led to a better thermal stability for the *P. koraiensis* lignin. Compared with the *P. koraiensis* and bagasse lignins, the eucalyptus lignin had a higher elemental oxygen content and lower molecular weight with mainly S-type structural units.

ACKNOWLEDGMENTS

The authors are grateful for the support of the National Key R&D project of China (Grant No. 2017YFB0307901) and the National Natural Science Foundation of China (Grant No. 21476091). The authors also appreciate the financial support from the Science and Technology Planning Project of Guangdong Province (Grant No. 2015A020215009) and the Science and Technology Planning Project of FoShan in Guangdong Province (Grant No. 2015AG10011).

REFERENCES CITED

Asmadi, M., Kawamoto, H., and Saka, S. (2011a). "Thermal reactivities of catechols/pyrogallols and cresols/xylenols as lignin pyrolysis intermediates," *J. Anal. Appl. Pyrol.* 92(1), 76-87. DOI: 10.1016/j.jaap.2011.04.012

Asmadi, M., Kawamoto, H., and Saka, S. (2011b). "Thermal reactions of guaiacol and syringol as lignin model aromatic nuclei," *J. Anal. Appl. Pyrol.* 92(1), 88-98. DOI: 10.1016/j.jaap.2011.04.011

Bansode, R. R., Losso, J. N., Marshall, W. E., Rao, R. M., and Portier, R. J. (2004). "Pecan shell-based granular activated carbon for treatment of chemical oxygen demand (COD) in municipal wastewater," *Bioresource Technol.* 94(2), 129-135. DOI: 10.1016/j.biortech.2003.12.009

Barker, D. J., Mannucchi, G. A., Salvi, S. M. L., and Stuckey, D. C. (1999). "Characterization of soluble residual chemical oxygen demand (COD) in anaerobic wastewater treatment effluents," *Water Res.* 33(11), 2499-2510. DOI: 10.1016/S0043-1354(98)00489-8

Britt, P. F., Kidder, M. K., and Buchanan III, A. C. (2007). "Oxygen substituent effects in the pyrolysis of phenethyl phenyl ethers," *Energ. Fuel.* 21(6), 3102-3108. DOI: 10.1021/ef700354y

Capanema, E. A., Balakshin, M. Y., and Kadla, J. F. (2004). "A comprehensive approach for quantitative lignin characterization by NMR spectroscopy," *J. Agr. Food Chem.* 52(7), 1850-1860. DOI: 10.1021/jf035282b

Canadian Journal of Chemical Engineering (1987). "Chemical engineering research and design," *Can. J. Chem. Eng.* 65(3), 528. DOI: 10.1002/cjce.5450650331

Ghaffar, S. H, and Fan, M. (2014). "Lignin in straw and its applications as an adhesive," *Int. J. Adhes. Adhes.* 48, 92-101. DOI: 10.1016/j.ijadhadh.2013.09.001

Hodgson, E. M., Nowakowski, D. J., Shield, I., Riche, A., Bridgwater, A. V., Clifton-Brown, J. C., and Donnison, I. S. (2011). "Variation in *Miscanthus* chemical composition and implications for conversion by pyrolysis and thermo-chemical bio-refining for fuels and chemicals," *Bioresource Technol.* 102(3), 3411-3418. DOI: 10.1016/j.biortech.2010.10.017

Huang, J.-b., Liu, C., Ren, L.-r., Tong, H., Li, W.-m., and Wu, D. (2013). "Studies on pyrolysis mechanism of syringol as lignin model compound by quantum chemistry," *Journal of Fuel Chemistry Technology* 41(6), 657-666. DOI: 10.1016/S1872-5813(13)60031-6

Karichappan, T., Venkatachalam, S., and Jeganathan, P. M. (2014). "Analysis of efficiency of *Bacillus subtilis* to treat bagasse based paper and pulp industry wastewater - A novel approach," *Journal of the Korean Chemical Society* 58(2), 198-204. DOI: 10.5012/jkcs.2014.58.2.198

Kumar, R., Singh, S., and Singh, O. V. (2009). "ChemInform abstract: Bioconversion of lignocellulosic biomass: Biochemical and molecular perspectives," *ChemInform* 40(28). DOI: 10.1002/chin.200928268

Laurichesse, S., Huillet, C, and Averous, L. (2014). "Original polyols based on organosolv lignin and fatty acids: New bio-based building blocks for segmented polyurethane synthesis," *Green Chem*. 16(8), 3958-3970. DOI: 10.1039/C4GC00596A

Lei, L., Chen, S., and Li, Y. (2013). "Effect of biological treatment on characteristics of soluble organic compounds in hardwood KP bleaching effluent," *BioResources* 8(3), 4349-4358. DOI: 10.15376/biores.8.3.4349-4358

Lucas, M. S., Peres, J. A., Amor, C., Prietorodríguez, L., Maldonado, M. I., and Malato, S. (2012). "Tertiary treatment of pulp mill wastewater by solar photo-Fenton," *J. Hazard Mater.* 225-226(2Pt1), 173-181. DOI: 10.1016/j.jhazmat.2012.05.013

Martínez, A. T., Speranza, M., Ruiz-Dueñas, F. J., Ferreira, P., Camarero, S., Guillén, F., Martínez, M. J., Gutiérrez, A., and del Río, J. C. (2005). "Biodegradation of lignocellulosics: Microbial, chemical, and enzymatic aspects of the fungal attack of lignin," *Int. Microbiol.* 8(3), 195-204.

Ohra-aho, T., Gomes, F. J. B., Colodette, J. L., and Tamminen, T. (2013). "S/G ratio and lignin structure among eucalyptus hybrids determined by Py-GC/MS and nitrobenzene oxidation," *J. Anal. Appl. Pyrol.* 101, 166-171. DOI: 10.1016/j.jaap.2013.01.015

Parthasarathi, R., Romero, R. A., Redondo, A., and Gnanakaran, S. (2011). "Theoretical study of the remarkably diverse linkages in lignin," *J. Phys. Chem. Lett.* 2(20), 2660-2666. DOI: 10.1021/jz201201q

Pasquali, C. E. L., and Herrera, H. (1997). "Pyrolysis of lignin and IR analysis of residues," *Thermochim. Acta* 293(1–2), 39-46. DOI: 10.1016/S0040-6031(97)00059-2

Rohella, R. S., Sahoo, N., Paul, S. C., Choudhury, S., and Chakravortty, V. (1996). "Thermal studies on isolated and purified lignin," *Thermochim. Acta* 287(1), 131-138. DOI: 10.1016/0040-6031(96)02983-8

Salem, M. Z. M., and Böhm, M. (2013). "Understanding of formaldehyde emissions from solid wood: An overview," *BioResources* 8(3), 4775-4790. DOI: 10.15376/biores.8.3.4775-4790

Santos, R. B., Capanema, E. A., Balakshin, M. Y., Chang, H.-m., and Jameel, H. (2012). "Lignin structural variation in hardwood species," *J. Agr. Food Chem.* 60(19), 4923-4930. DOI: 10.1021/jf301276a

Sun, R. C., Tomkinson, J., and Jones, G. L. (2000). "Fractional characterization of ash-AQ lignin by successive extraction with organic solvents from oil palm EFB fibre," *Polym. Degrad. Stabil*. 68(1), 111-119. DOI: 10.1016/S0141-3910(99)00174-3

Vanholme, R., Demedts, B., Morreel, K., Ralph, J., and Boerjan, W. (2010). "Lignin biosynthesis and structure," *Plant Physiol.* 153(3), 895-905. DOI: 10.1104/pp.110.155119

Wu, S.-b., Xiang, B.-l., Liu, J.-y., Guo, Y.-l., and Sun, R.-c. (2008). "Pyrolysis characteristics of technical alkali lignin," *Journal of Beijing Forestry University* 30(05), 143-147.

Article submitted: June 27, 2018; Peer review completed: August 22, 2018; Revised version received and accepted: August 30, 2018; Published: October 26, 2018.
DOI: 10.15376/biores.13.4.9053-9065